



**HAL**  
open science

# Estimation of inverter voltage disturbances for induction machine drive using LPV observer with convex optimization

Xuefang Lin-Shi, Paolo Massioni, Jean-Yves Gauthier

► **To cite this version:**

Xuefang Lin-Shi, Paolo Massioni, Jean-Yves Gauthier. Estimation of inverter voltage disturbances for induction machine drive using LPV observer with convex optimization. *Mathematics and Computers in Simulation*, 2021, 184, pp.196-209. 10.1016/j.matcom.2020.06.004 . hal-02955229

**HAL Id: hal-02955229**

**<https://hal.science/hal-02955229>**

Submitted on 3 Feb 2023

**HAL** is a multi-disciplinary open access archive for the deposit and dissemination of scientific research documents, whether they are published or not. The documents may come from teaching and research institutions in France or abroad, or from public or private research centers.

L'archive ouverte pluridisciplinaire **HAL**, est destinée au dépôt et à la diffusion de documents scientifiques de niveau recherche, publiés ou non, émanant des établissements d'enseignement et de recherche français ou étrangers, des laboratoires publics ou privés.



Distributed under a Creative Commons Attribution - NonCommercial 4.0 International License

# Estimation of inverter voltage disturbances for induction machine drive using LPV observer with convex optimization

Xuefang Lin-Shi<sup>a,b</sup>, Paolo Massioni<sup>a</sup>, Jean-Yves Gauthier<sup>a</sup>

<sup>a</sup>*Laboratoire Ampère, UMR CNRS 5005, INSA Lyon, Université de Lyon, F-69621 Villeurbanne, France*

<sup>b</sup>*School of Electronics and Information Engineering, Tianjin Polytechnic University, 300387, Tianjin, China*

---

## Abstract

This paper presents a Linear Parameter-Varying (LPV) observer for an Induction Machine (IM) under sinusoidal DC-supply disturbances. The observer estimates not only the IM state variables, but also the disturbances considered as a part of the states. As the extended IM model depends on the stator angular speed  $\omega_s$  and the rotor angular speed  $\omega_r$ , the proposed observer is designed by convex optimization to induce a convergence of the observer for a predetermined range of  $\omega_s$  and  $\omega_r$ . The estimated disturbances can be used to compensate for the real disturbances. The simulation results show the effectiveness of the observer, and experimental results on a laboratory test-bench have been obtained. The proposed method can be extended to other type of motor drives.

*Keywords:* Electrical drive, Linear Parameter Varying (LPV) observer, convex optimization, inverter voltage disturbance.

---

## 1. Introduction

Electrical drive is widely used in industrial applications such as renewable energy generation, electrical vehicles or railway traction. The quality of the

---

*Email addresses:* [xuefang.shi@insa-lyon.fr](mailto:xuefang.shi@insa-lyon.fr) (Xuefang Lin-Shi), [paolo.massioni@insa-lyon.fr](mailto:paolo.massioni@insa-lyon.fr) (Paolo Massioni), [jean-yves.gauthier@insa-lyon.fr](mailto:jean-yves.gauthier@insa-lyon.fr) (Jean-Yves Gauthier)

*Preprint submitted to Mathematics and Computers in Simulation*

*May 3, 2020*

controlled currents or torque is primordial. An electrical machine is driven by an inverter which is supplied by a DC voltage. This last can be obtained from an alternative source through a power factor correction (PFC) rectifier for example. In this case, the inherent ripple power at twice the line frequency is injected into the DC side of the PFC. This can induce many harmonics in the DC voltage. It is reported in [1] that the principal harmonic found on the DC voltage is the second harmonic of the line voltage. This last can be assimilated by a sinusoidal disturbance whose frequency is known. In a controlled environment, the DC supply disturbances of the inverter can induce disturbances of the control voltages and thus degrade the quality of controlled currents and lead to ripples of the torque. This paper focuses on the control disturbances for one given harmonic induced by the inverter supply. When the control disturbances can be assimilated to a sinusoidal waveforms with known frequencies, they can be considered as a part of the states [2]. An observer can then be used to estimate and compensate for it. Tebbani and coworkers [3] use a Kalman filter to reduce output low-frequency ripples that appear on the control voltage in a train supply application. In [2], active reduction of vibrations in synchronous motors by using a Luenberger observer has been presented. This last is designed for a single operation point, with the consequence that the stability can not be guaranteed for all speed range. Since the performance of the observer depends on the stator rotational speed  $\omega_s$  and the rotor rotational speed  $\omega_r$  of the machine, the determination of the observer gain has always been a topic of interest.

Some results in the field of robust estimation have highlighted new possibilities: Linear Parameter Varying (LPV) observer gains can be designed to minimize a  $L_2$ -gain (energy gain) or  $H_\infty$  norm on the estimation error [4, 5]. This approach is alternative to the one based on minimizing the variance of the estimation error, which is at the foundation of the stochastic approach of the Kalman filter [6].

In this paper, we propose a stabilising LPV observer of an IM by taking into account the sinusoidal waveform disturbances with known frequencies. These disturbances can be modeled as a part of the states. The methodology is applicable for other types of electrical motors such as synchronous motors. A systematic method is presented to design the gains of the observer off-line considering a given range for the stator and the rotor speed of the IM. These gains are computed by convex optimization, and they guarantee the convergence of the observer for all the speeds in the defined range. The observer estimates not only the IM state variables, but also the harmonics

coming from the control voltage disturbances, in order to make it possible to perform an active compensation to reduce the effect of these disturbances.

The paper is organized as follows. Section 2 presents first the IM model, then the disturbance modelling for one harmonic induced by the DC-voltage. An extended LPV model is thus obtained which depends on the disturbance frequency  $\omega_d$ , the angular frequency of the stator  $\omega_s$  and rotor  $\omega_r$ . The observability of the extended model is analyzed as well in the same section. Section 3 contains the description of the systematic gain design method. Section 4 presents the simulation results for the designed observer performed with an industrial used induction, whereas Section 5 presents some experimental results validated in a laboratory test bench.

## 2. Extended IM model including voltage disturbances

### 2.1. IM Modelling

By assuming that the saturation of the magnetic parts and the hysteresis phenomenon are neglected, the dynamical model of the electrical part of an induction motor in the rotating reference frame  $(d, q)$  can be written by means of the following equations [7]:

$$\begin{cases} \dot{X} = A(\omega_s, \omega_r) X + BU \\ y = CX \end{cases} \quad (1)$$

with  $X = [i_{sd}, i_{sq}, \varphi_{rd}, \varphi_{rq}]^T$ ,  $U = [u_{sd}, u_{sq}]^T$ ,  $Y = [i_{sd}, i_{sq}]^T$ ,

$$A(\omega_s, \omega_r) = \begin{bmatrix} -\left(\frac{R_s}{L_\sigma} + \frac{L_m^2 R_r}{L_\sigma L_r^2}\right) & \omega_s & \frac{L_m R_r}{L_\sigma L_r^2} & \frac{L_m \omega_r}{L_\sigma L_r} \\ -\omega_s & -\left(\frac{R_s}{L_\sigma} + \frac{L_m^2 R_r}{L_\sigma L_r^2}\right) & \frac{L_m \omega_r}{L_\sigma L_r} & \frac{L_m R_r}{L_\sigma L_r^2} \\ \frac{L_m R_r}{L_r} & 0 & -\frac{R_r}{L_r} & (\omega_s - \omega_r) \\ 0 & \frac{L_m R_r}{L_r} & -(\omega_s - \omega_r) & -\frac{R_r}{L_r} \end{bmatrix},$$

$$B = \begin{bmatrix} \frac{1}{L_\sigma} & 0 & 0 & 0 \\ 0 & \frac{1}{L_\sigma} & 0 & 0 \end{bmatrix}^T, \quad C = \begin{bmatrix} 1 & 0 & 0 & 0 \\ 0 & 1 & 0 & 0 \end{bmatrix},$$

where  $(i_{sd}, i_{sq})$  are the stator currents in the rotating  $(d, q)$  reference frame,  $(\varphi_{rd}, \varphi_{rq})$  are the rotor fluxes in the same reference,  $(u_{sd}, u_{sq})$  are the stator voltages,  $R_r$  is the rotor resistance,  $R_s$  is the stator resistance;  $L_r$ ,  $L_m$  and  $L_\sigma$  are respectively the rotor, magnetizing and leakage inductances, and  $\omega_s$  and  $\omega_r$  are respectively the angular frequency of the stator currents and rotor flux.

## 2.2. Disturbance modelling

Generally an IM is driven by a three-phase inverter which is supplied by a DC-voltage obtained by an AC/DC converter such as a PFC rectifier. Fig. 1 shows a basic PFC topology to generate the DC-voltage of the three-phase inverter. The DC-voltage quality depends on the PFC topology and its control [8] which are out of scope of this paper. However, it can be considered that the voltage contains many harmonics where their frequency can be identified but their amplitude can evolve with the load power. These harmonics with unknown amplitude can be taken into account in a disturbance model as follows.

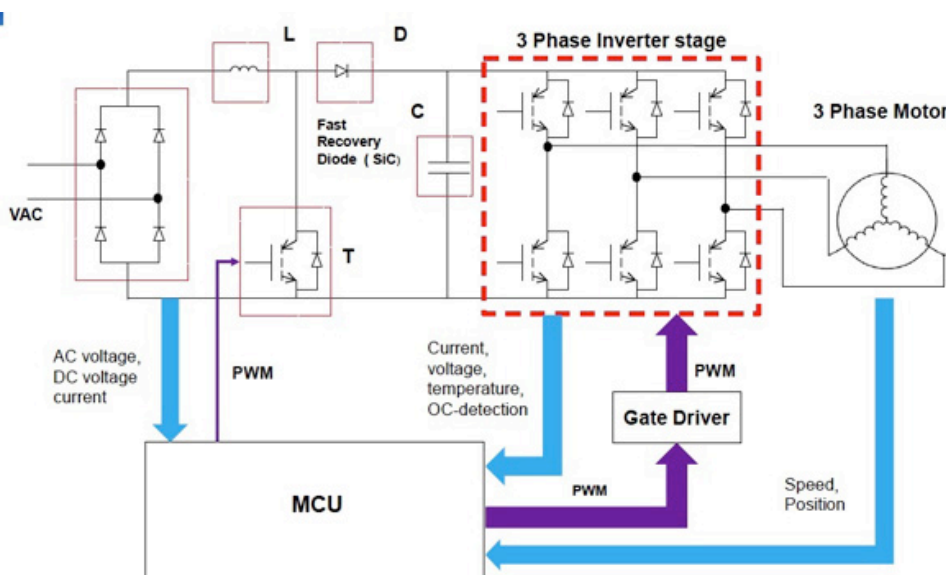


Figure 1: PFC stage for a motor controller [9].

For the sake of simplicity, we take one harmonic with angular frequency of  $\omega_d$  rad/s as example. It can be extended for other harmonics with the same principle. As it will be shown in section 4.1, a sinusoidal waveform disturbance on DC supply of the inverter induce the control voltage disturbances with the same frequency. The corresponding disturbances on the stator voltages in the  $(d,q)$  reference frame are two sinusoidal waveform disturbances with the same angular frequency. Without loss of generality, these disturbances are modeled as two sinusoidal waveforms  $d_d = D_{d0} \sin(\omega_d t + \phi_d)$  and

$d_q = D_{q0} \sin(\omega_d t + \phi_q)$ . These disturbances can be written in state-space form:

$$X_d = \begin{bmatrix} D_{d0} \sin(\omega_d t + \phi_d) \\ D_{d0} \cos(\omega_d t + \phi_d) \\ D_{q0} \sin(\omega_d t + \phi_q) \\ D_{q0} \cos(\omega_d t + \phi_q) \end{bmatrix} \quad (2)$$

$$\dot{X}_d = \begin{bmatrix} 0 & \omega_d & 0 & 0 \\ -\omega_d & 0 & 0 & 0 \\ 0 & 0 & 0 & \omega_d \\ 0 & 0 & -\omega_d & 0 \end{bmatrix} X_d = A_d(\omega_d) X_d$$

The same principle can be used to add other disturbance harmonics in the disturbance model.

### 2.3. Extended Model

By taking into account the disturbance model (2) in the IM model (2.1), an augmented model of order 8 can be obtained as follows [2]:

$$\begin{cases} \dot{X}_e = A_e(\omega_d, \omega_s, \omega_r) X_e + B_e U \\ Y = C_e X_e \end{cases} \quad (3)$$

with

$$X_e = [X, X_d]^T$$

$$A_e = \begin{bmatrix} A(\omega_s, \omega_r) & BC_d \\ 0_{4 \times 4} & A_d(\omega_d) \end{bmatrix}, \quad B_e = \begin{bmatrix} B \\ 0_{4 \times 2} \end{bmatrix}$$

$$C_d = \begin{bmatrix} 1 & 0 & 0 & 0 \\ 0 & 0 & 1 & 0 \end{bmatrix}$$

$$C_e = \begin{bmatrix} 1 & 0 & 0 & 0 & 0 & 0 & 0 & 0 \\ 0 & 1 & 0 & 0 & 0 & 0 & 0 & 0 \end{bmatrix}.$$

This model is a LPV system depending on the stator and rotor speed of the IM and on the identified disturbance frequency  $\omega_d$ . It can be noted that the disturbance here is not to be taken as an unknown input, but rather as a part of the state-space vector which will be estimated by a LPV observer.

#### 2.4. Observability analysis

A LPV observer will be developed in order to retrieve all the states of  $X_e$  from the current measurements. Before designing an observer for the system (3), it is necessary to study the system's observability by using the criterion developed by Kalman [10]. The observability of the LPV systems may be evaluated by analyzing the rank condition of the observability matrix according to  $\omega_d$ ,  $\omega_s$  and  $\omega_r$ .

The observability matrix is expressed as:

$$O_e(\omega_d, \omega_s, \omega_r) = [ C_e \quad C_e A_e \quad C_e A_e^2 \quad \dots \quad C_e A_e^7 ]^T \quad (4)$$

The rank condition is satisfied if it is possible to find a submatrix  $O(\omega_d, \omega_s, \omega_r)$  of size  $8 \times 8$  inside the observability matrix  $O_e(\omega_d, \omega_s, \omega_r)$  which has a non-zero determinant. It turns out that the determinant of the upper block of the observability matrix is given by:

$$\det[O(\omega_d, \omega_s, \omega_r)] = -\left(\frac{1}{L\sigma}\right)^4 \left(\frac{L_m}{L\sigma L_r}\right)^2 \omega_d^2 \left( \left(\frac{R_r}{L_r}\right)^2 + \omega_r^2 \right) \left( \left( \left(\frac{R_r}{L_r}\right)^2 + \omega_d^2 - (\omega_r - \omega_s)^2 \right)^2 + 4\left(\frac{R_r}{L_r}\right)^2 (\omega_r - \omega_s)^2 \right) \quad (5)$$

This determinant is different from zero for any value of  $\omega_s$  and  $\omega_r$  if  $\omega_d \neq 0$ . The system (3) is therefore observable when  $\omega_d \neq 0$ . When  $\omega_d = 0$ , it means that the disturbance inputs are constants; it is then easy to observe these disturbances as proposed in [2].

### 3. LPV Observer Design

The design of the observer can be done by numerical convex optimisation. The method proposed here is inspired by the approach of [11] and [12], and it is based on the concept of regional pole placement described in [13]; in this sense, it is very different from the approach in [4, 5], which is based on  $H_\infty$  performance.

The goal of this observer is to create a state dynamics for a variable  $\hat{X}_e$  such that  $\hat{X}_e$  tends to  $X_e$  asymptotically. Assuming the parameters  $\omega_d$ ,  $\omega_s$ , and  $\omega_r$  to be known at all times, then the standard observer dynamics, for

(3), are given by the equations

$$\begin{cases} \dot{\hat{X}}_e = A_e(\omega_d, \omega_s, \omega_r)\hat{X}_e - K(\omega_d, \omega_s, \omega_r)(Y - \hat{Y}) + B_e U \\ \hat{Y} = C_e \hat{X}_e \end{cases} \quad (6)$$

where  $K(\omega_d, \omega_s, \omega_r)$  is a parameter-dependent observer gain, to be determined. This is a LPV observer due to the dependence of the gain on the parameters. Expressing the observer error  $E$  as  $\hat{X}_e - X_e$ , as a consequence of (6) and (3) its dynamics are described by

$$\dot{E} = (A_e(\omega_d, \omega_s, \omega_r) - K(\omega_d, \omega_s, \omega_r)C_e)E. \quad (7)$$

The error dynamics are asymptotically stable (i.e. the error converges to zero) if there exists a positive definite Lyapunov matrix  $P$  such that

$$\begin{aligned} & P(A_e(\omega_d, \omega_s, \omega_r) - K(\omega_d, \omega_s, \omega_r)C_e) \\ & + (A_e(\omega_d, \omega_s, \omega_r) - K(\omega_d, \omega_s, \omega_r)C_e)^\top P < 0 \end{aligned} \quad (8)$$

for all  $\omega_s \in [\underline{\omega}_s, \overline{\omega}_s]$  and  $\omega_r \in [\underline{\omega}_r, \overline{\omega}_r]$ , and for a constant  $\omega_d$ . The expression above can be used to find a stabilising observer gain  $K(\omega_d, \omega_s, \omega_r)$ ; in this case, both  $P$  and  $K(\omega_d, \omega_s, \omega_r)$  are unknown and the inequality is nonlinear in the decision variables. With a given constant  $\omega_d$ , assuming that  $K(\omega_d, \omega_s, \omega_r) = K(\omega_s, \omega_r)$  is linear in the parameters, i.e.  $K(\omega_s, \omega_r) = K_0 + K_{\omega_s}\omega_s + K_{\omega_r}\omega_r$ , the change of variables  $L(\omega_s, \omega_r) = PK(\omega_s, \omega_r) = PK_0 + PK_{\omega_s}\omega_s + PK_{\omega_r}\omega_r$  allows reformulating (8) as

$$\begin{aligned} & PA_e(\omega_d, \omega_s, \omega_r) - L(\omega_s, \omega_r)C_e \\ & + A_e(\omega_d, \omega_s, \omega_r)^\top P - C_e^\top L(\omega_s, \omega_r)^\top < 0, \end{aligned} \quad (9)$$

which is a parameter-dependent LMI (linear matrix inequality) [14]. The dependence on the parameters is linear (also called polytopic), so it can be removed by simply reformulating the inequality for all the extreme values of the parameters. This means that a stabilising parameter-dependent observer

gain  $K(\omega_s, \omega_r)$  can be found by solving

$$\begin{aligned}
& P > 0, \\
& PA_e(\omega_d, \overline{\omega_s}, \overline{\omega_r}) - L(\overline{\omega_s}, \overline{\omega_r}) C_e \\
& + A_e(\omega_d, \overline{\omega_s}, \overline{\omega_r})^\top P - C_e^\top L(\overline{\omega_s}, \overline{\omega_r})^\top < 0, \\
& PA_e(\omega_d, \overline{\omega_s}, \underline{\omega_r}) - L(\overline{\omega_s}, \underline{\omega_r}) C_e \\
& + A_e(\omega_d, \overline{\omega_s}, \underline{\omega_r})^\top P - C_e^\top L(\overline{\omega_s}, \underline{\omega_r})^\top < 0, \tag{10} \\
& PA_e(\omega_d, \underline{\omega_s}, \overline{\omega_r}) - L(\underline{\omega_s}, \overline{\omega_r}) C_e \\
& + A_e(\omega_d, \underline{\omega_s}, \overline{\omega_r})^\top P - C_e^\top L(\underline{\omega_s}, \overline{\omega_r})^\top < 0, \\
& PA_e(\omega_d, \underline{\omega_s}, \underline{\omega_r}) - L(\underline{\omega_s}, \underline{\omega_r}) C_e \\
& + A_e(\omega_d, \underline{\omega_s}, \underline{\omega_r})^\top P - C_e^\top L(\underline{\omega_s}, \underline{\omega_r})^\top < 0,
\end{aligned}$$

for  $P$  and  $L(\omega_s, \omega_r)$ , and then  $K(\omega_s, \omega_r) = P^{-1}L(\omega_s, \omega_r)$ . LMIs can be solved using appropriate software, in this case we have relied on Matlab's Mosek implementation [15], coded through Yalmip [16]. Note that the larger the range of  $\omega_s$  and  $\omega_r$ , the less efficient the observer will be.

The LMI conditions in (10) only assure that the observer is stable, but it is interesting to add additional constraints in order to impose certain limits to the closed-loop dynamics. For example, just imposing the stability will not put any constraints on how fast the convergence will happen, or how damped or oscillating the observer dynamics will be. This can instead be imposed if the closed loop poles are constrained into a region as in Fig. 2, where 1) the minimum value of the real part of the poles ( $\alpha_{min}$ ) imposes a minimum rate of convergence, 2) the maximum value ( $\alpha_{max}$ ) limits the speed of the convergence (this is necessary as the closed-loop poles must be slower than the Shannon frequency of the real-time control system, and also preferably slower than the measurement noise), and 3) the sector condition (depending on the slope  $\beta$ ) assures a minimum damping level to the poles. These conditions, as explained in [13], are assured by solving the following

LMI problem:

$$\begin{aligned}
& P > 0, \\
& PA_e - LC_e + A_e^\top P - C_e^\top L^\top + 2P\alpha_{min} \leq 0, \\
& PA_e - LC_e + A_e^\top P - C_e^\top L^\top + 2P\alpha_{max} \geq 0, \\
& \begin{bmatrix} \beta(A_e^\top P - C_e^\top L^\top + PA_e - LC_e) & A_e^\top P - C_e^\top L^\top - PA_e + LC_e \\ -A_e^\top P + C_e^\top L^\top + PA_e - LC_e & \beta(A_e^\top P - C_e^\top L^\top + PA_e - LC_e) \end{bmatrix} \leq 0,
\end{aligned} \tag{11}$$

where the parametric dependence of the variables has been dropped for brevity, i.e. read  $A_e(\omega_d, \omega_s, \omega_r)$  for  $A_e$  and  $L(\omega_d, \omega_s, \omega_r)$  for  $L$ . By assuming again a linear expression of the observer gain as a function of the parameters, i.e.  $K(\omega_d, \omega_s, \omega_r) = K(\omega_s, \omega_r)$ , the problem is solved by running the optimisation for the four vertices of the polytope  $(\omega_s, \omega_r)$ , as done in (10) for (9).

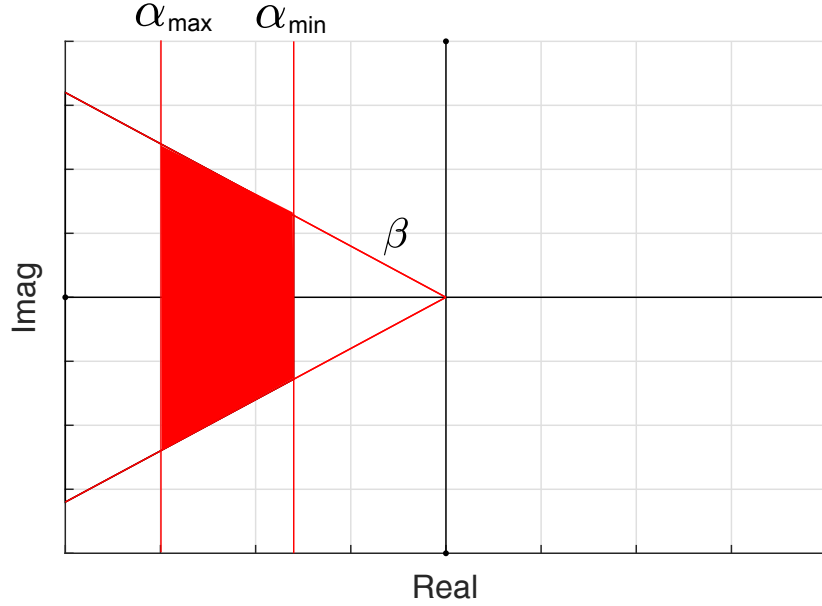


Figure 2: Pole placement constraints.

Table 1: Simulation Induction machine parameters.

Electrical parameters			
$N_p$	number of pole pairs		2
$R_r$	rotor resistance		1.179 $\Omega$
$R_s$	stator resistance		1 $\Omega$
$L_r$	rotor inductance		0.1197 H
$L_m$	magnetizing inductance		0.1197 H
$L_\sigma$	leakage inductance		27.6 mH
Nominal values			
$P_{nom}$	nominal power		1.8 kW
$I_{nom}$	nominal current		4 A
$V_{nom}$	nominal voltage		326 V
$\varphi_{nom}$	nominal flux		0.52 Wb
$\Omega_{nom}$	nominal speed		1420 rpm
$T_{e\,nom}$	nominal torque		12.1 Nm

#### 4. Simulation results

The proposed LPV observer has been first validated in simulations. The machine used for simulation studies is an industrial 1.8 kW induction machine whose parameters are presented in Tab. 1.

##### 4.1. Simulation conditions

First the scheme presented in Fig. 3 is simulated with Matlab / Simulink where the inverter averaged model is introduced. The behaviour of the PFC rectifier is not simulated in detail since it takes more simulation time. Only one harmonic with  $\omega_d = 50\text{Hz}$  of 30V amplitude as example is added on the DC voltage in front of the inverter.

A classical field-oriented control [17] is considered. For a speed changed between 0 and 800 rpm, Fig. 4 shows the difference between the control voltage  $u_{sd}$  (respectively  $u_{sq}$ ) and the disturbed control voltage  $u_{sdp}$  (respectively  $u_{sqp}$ ) calculated from the voltages  $u_{ap}$ ,  $u_{bp}$  and  $u_{cp}$  delivered by the inverter. These differences noted  $d_d$ ,  $d_q$  are two sinusoidal waveform disturbances with the same frequency as that of the DC-supply disturbance. It confirms our disturbance model in Section 2.

In order to accelerate the simulation time, the model of the inverter is suppressed thereafter. The DC supply disturbances are taken into account

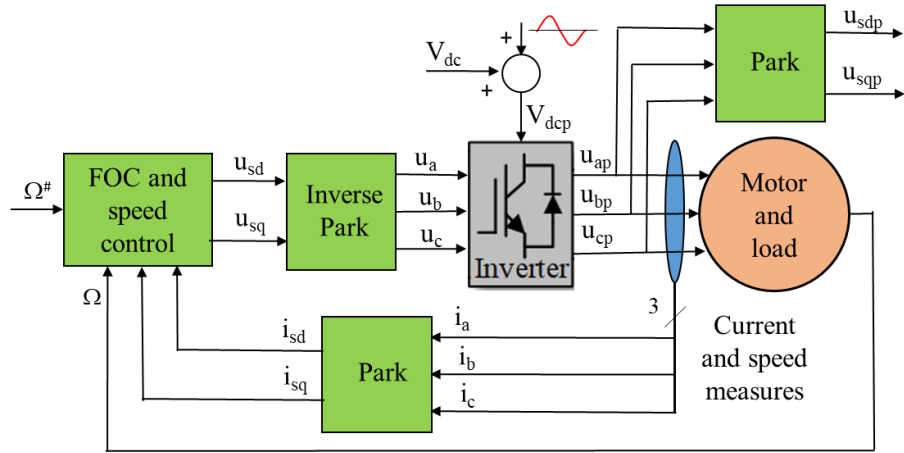


Figure 3: Classical field-oriented control with supply disturbance

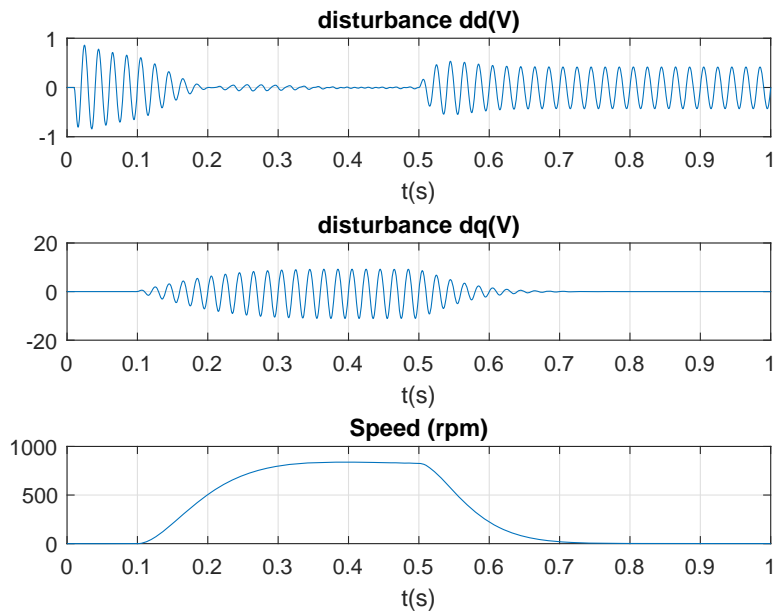


Figure 4: Influence of inverter supply disturbance on the control voltage

in the simulation by adding sinusoidal waveform disturbances  $d_d$  and  $d_q$  to control voltages  $u_{sd}$  and  $u_{sq}$  as shown in Fig. 5. Without loss of gen-

erality, two sinusoidal waveform disturbances  $d_d = D_{d0}\sin(\omega_d t + \phi_d)$  and  $d_q = D_{q0}\sin(\omega_d t + \phi_q)$  have been introduced in the simulation for different  $\omega_d$ .

The speed ranges for observer design are  $\omega_s \in [0, 320]$  rad/s and  $\omega_r \in [0, 320]$  rad/s. These worst-case ranges are willingly chosen for simulations. For negative values of speed, a second gain can also be determined.  $\alpha_{min}$  and  $\alpha_{max}$  are chosen as 0.5 rad/s and 50 rad/s respectively. The value of  $\alpha_{max}$  is way below the frequency of the noise, which we consider to be acting on frequency of the order of the kHz.

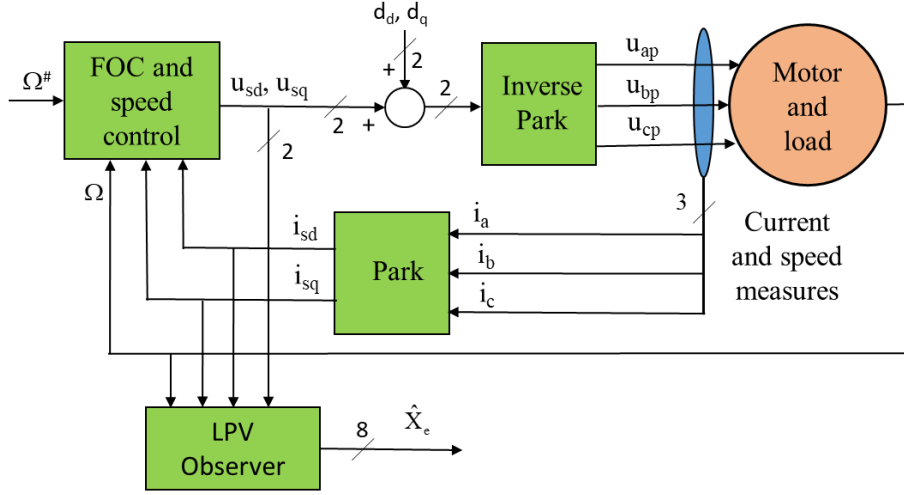


Figure 5: Field-oriented control with observer

#### 4.2. Open-loop state estimations

To verify the performance of the observer for different speeds, the motor is controlled from 0 to 1500 rpm. The flux remains constant at its nominal value. A load torque of  $T_l = 5$  Nm is applied at  $t = 4$  s. Two disturbances are tested, one with low frequency (1Hz) to better view the disturbance observation, the other with higher frequency (50Hz).

First, we take  $d_d = D_{d0}\sin(\omega_d t + \phi_d)$  and  $d_q = D_{q0}\sin(\omega_d t + \phi_q)$  with  $\omega_d = 2\pi$  rad/s,  $D_{d0} = D_{q0} = 10$  V,  $\phi_d = 0$  and  $\phi_q = \frac{\pi}{2}$ . From the measured speed  $\Omega$  and currents  $i_{sd}$  and  $i_{sq}$ , the observer estimates all the states of  $X_e$ , including the disturbances  $\hat{d}_d$  and  $\hat{d}_q$  with their amplitude and phase shift.

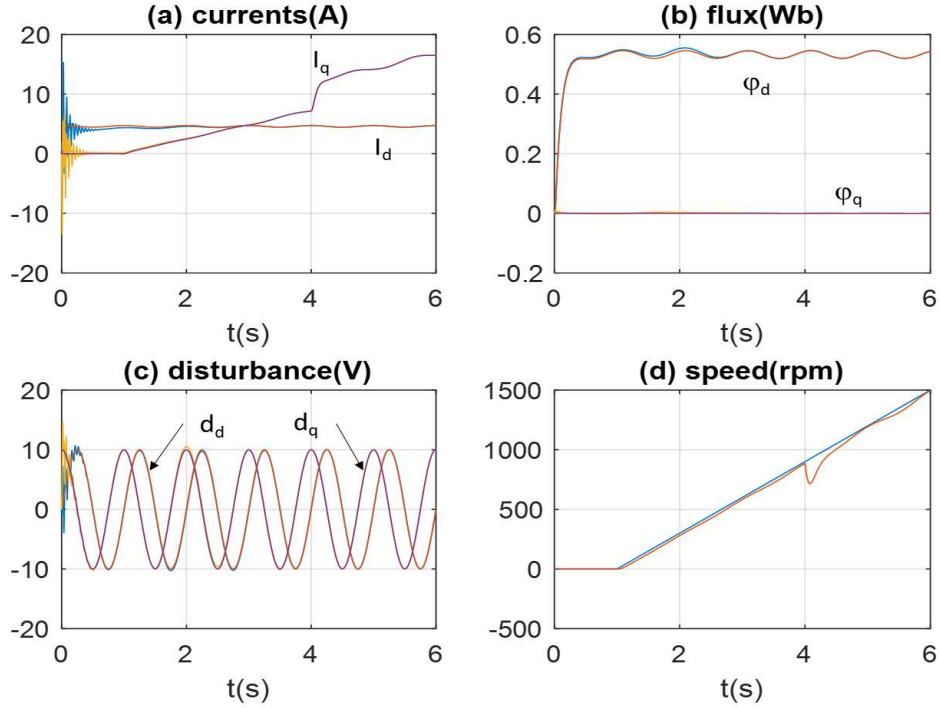


Figure 6: Comparison between the estimated states and the simulated ones for 1 Hz disturbances

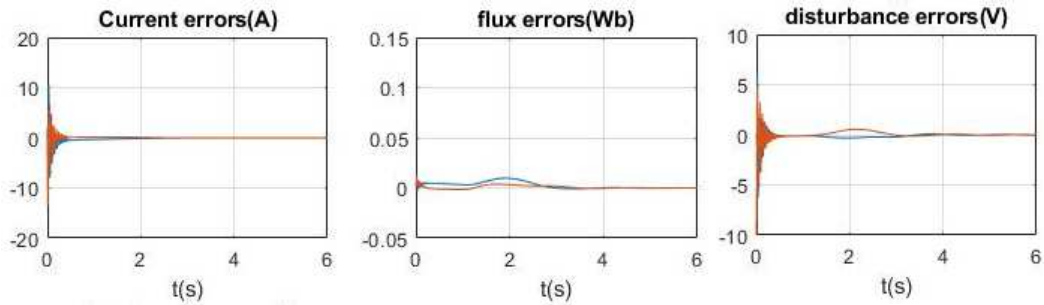


Figure 7: Observation error for 1Hz disturbances

Fig. 6 shows the comparison between the estimated currents, flux, disturbances and the simulated ones. The estimated states converge quickly. The speed evolution is presented in Fig. 6 (d). The observation errors are small for all the range of speeds (Fig. 7). The load torque has no influence

on the observation performance.

Second, we take  $\omega_d = 100\pi$  rad/s,  $D_{d0} = D_{q0} = 10$  V,  $\phi_d = 0$  and  $\phi_q = \frac{\pi}{2}$ .

The comparison between the estimated extended states and the simulated ones, and the observation errors, are shown respectively in Fig. 8 and Fig. 9. The observer converges quickly and the observation errors remain small.

More simulations with other disturbances for different  $\omega_d$ ,  $D_{d0}$ ,  $D_{q0}$ ,  $\phi_d$  and  $\phi_q$  give similar results. The estimation is quite accurate for all the states including the disturbances  $\hat{d}_d$  and  $\hat{d}_q$ .

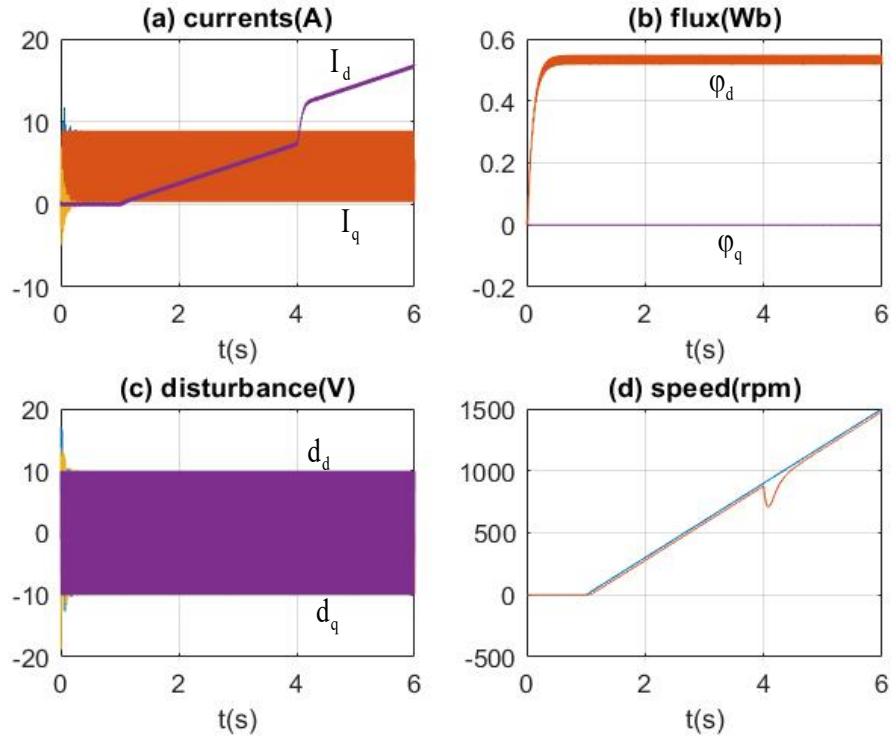


Figure 8: Comparison between the estimated states and the simulated ones for 50 Hz disturbances

#### 4.3. Disturbance compensations

From Fig. 8, it can be seen that the disturbances  $d_d$  and  $d_q$  cause oscillations in the currents  $i_{sd}$  and  $i_{sq}$ . These induce more losses and lead to torque oscillations. If these disturbances are well estimated by the proposed

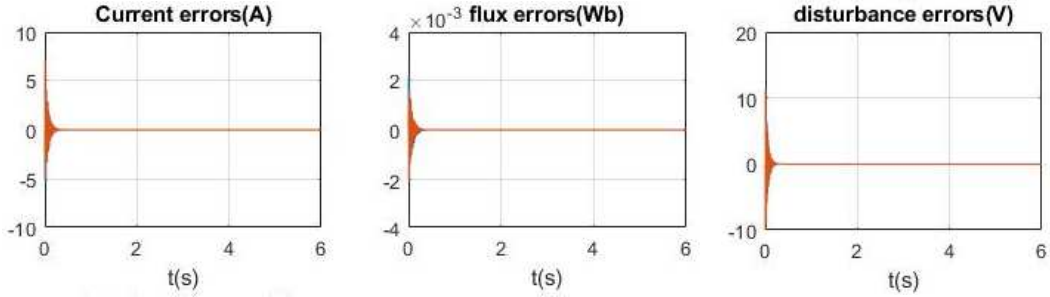


Figure 9: Observation error for 50Hz disturbances

observer, it is possible to compensate these disturbances by adding the opposite terms of  $\hat{d}_d$  and  $\hat{d}_q$  to the main controller outputs.

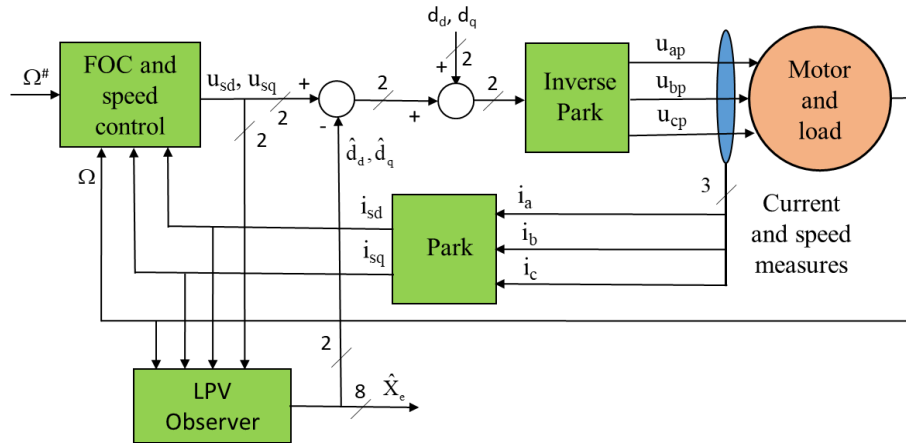


Figure 10: Disturbance compensation scheme

Fig. 10 is implemented to verify the feasibility of the disturbance compensation. A step response of the speed from 0 to 1000 rpm has been made without torque load. The disturbances are always sinusoidal waveforms with  $\omega_d = 100\pi$  rad/s,  $D_{d0} = D_{q0} = 10$  V,  $\phi_d = 0$  and  $\phi_q = \frac{\pi}{2}$ . The disturbance compensations are enabled at  $t = 2$  s. The estimated and simulated currents are shown in Fig. 11 (a) and the torque is presented in Fig. 11 (b). The estimated errors are not plotted because they are similar to Fig. 9. The benefit of using disturbance compensation can be observed through the difference between the cases with and without disturbance compensation.

The parameters of a motor are never perfectly identified. Moreover, these

parameters can evolve with temperature over time. It is interesting to study the robustness of the observer. First, the same simulation as for Fig. 11 has been made by adding 20% errors respectively on  $R_s$  and  $R_r$ . It can be seen from Fig. 12 that still the disturbance compensation works well (after 2 s) despite the static observation errors on  $d_d$  and  $d_q$  (Fig. 12 (c) and (d)).

Note that disturbance compensation must be made with care, notably when the inductances are badly identified. When a 20% error is introduced on  $L_r$ , not only are there estimation errors on the amplitude of the disturbances (Fig. 13 (a) and (b)), but a phase shift also appears between  $d_d$  and  $\hat{d}_d$  (Fig. 13 (c)). It is clear that when the phase shift exists, a compensation does not work well. So the disturbance compensations is not enabled in this simulation. From Fig. 13 (c), it is possible to remark that the amplitude of  $\hat{d}_d$  is smaller than that of  $d_d$  contrary to Fig. 13 (d) where  $\hat{d}_q$  overestimates  $d_q$ .

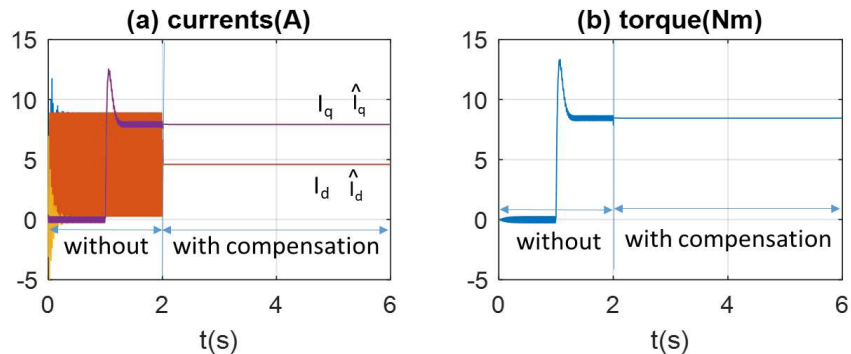


Figure 11: Disturbances compensation at 3s with nominal parameters

## 5. Experimental results

The field-oriented control and the LPV observer have been implemented on a dSPACE rapid control prototyping system using Simulink and the Real-time workshop toolbox of MATLAB. A laboratory test-bench has been used (Fig. 14). It is composed of one 13.6 W induction machine (EMsynergy) whose parameters are presented in Tab. 2. The inverter is supply by a 24V DC voltage generator. A 1000-pulse incremental encoder is used. The current are measured using three LEM current sensors. A permanent magnet

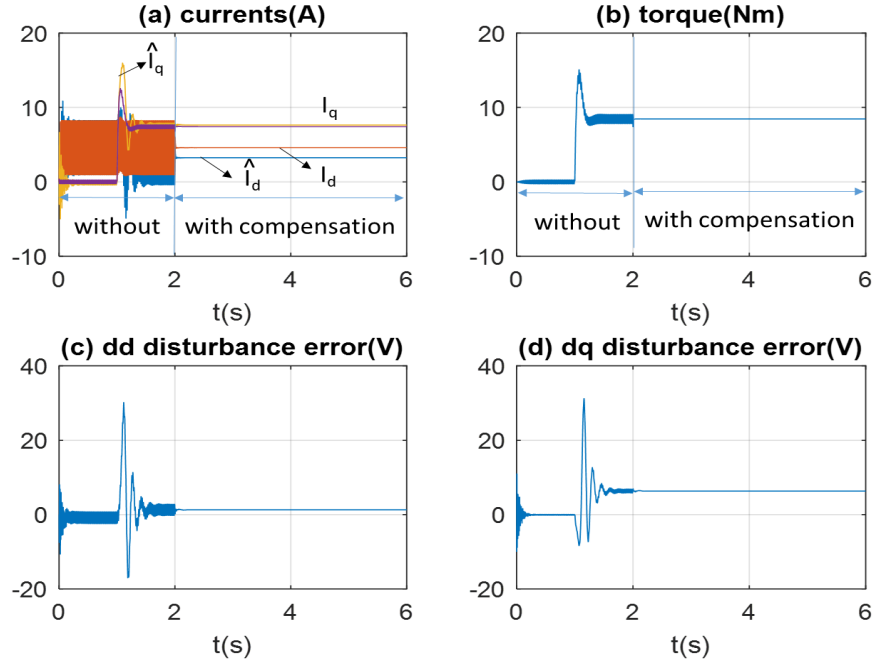


Figure 12: Disturbance compensations with 20% errors on  $R_s$  and  $R_r$ .

synchronous machine (PMSM) controlled by another dsPICDEM-MCLV-2 is used as load torque generator.

First, the speed is controlled to 100 rpm under a sinusoidal waveform disturbances on control voltage with  $\omega_d = 2\pi$  rad/s,  $D_{d0} = D_{q0} = 1$  V,  $\phi_d = 0$  and  $\phi_q = 0$ ; 25% of nominal torque has been applied. Fig. 15 shows the experimental results of the observed disturbances (red solid line) compared to injected ones (blue dashdot line). It can be seen that the disturbance  $d_q$  is well estimated. There is a small static error for the disturbance  $d_d$  estimation. This is due probably to the motor's parameters which are not well identified. It can be remarked too that the estimated disturbances are noisy since the measured currents are noisy contrary to simulation.

Then the speed reference is increased to 200 rpm. From Fig. 16, it can be seen that the disturbance  $d_q$  is always well estimated and the static error of the disturbance  $d_d$  estimation increase a little as the motor's parameters can evolve with temperature over time. As underlined in simulation, the disturbance compensation works well despite the static observation errors on  $d_d$  and  $d_q$ . We inject the estimated disturbances in the control voltage

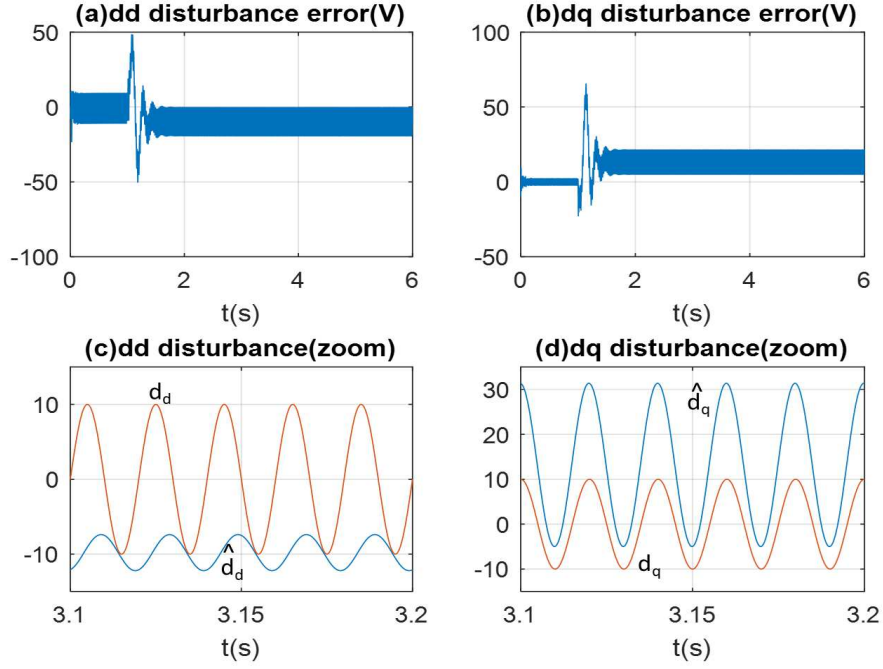


Figure 13: Disturbance estimations with 20% error on  $L_r$

Table 2: Experimental Induction machine parameters.  
Electrical parameters

$N_p$	number of pole pairs	2
$R_r$	rotor resistance	1.05 $\Omega$
$R_s$	stator resistance	1.79 $\Omega$
$L_r$	rotor inductance	28 mH
$L_m$	magnetizing inductance	30 mH
$L_\sigma$	leakage inductance	6.81 mH
Nominal values		
$P_{nom}$	nominal power	13.6 W
$I_{nom}$	nominal current	2 A
$V_{nom}$	nominal voltage	24 V
$\varphi_{nom}$	nominal flux	0.03 Wb
$\Omega_{nom}$	nominal speed	1121 rpm
$T_{e nom}$	nominal torque	0.116 Nm

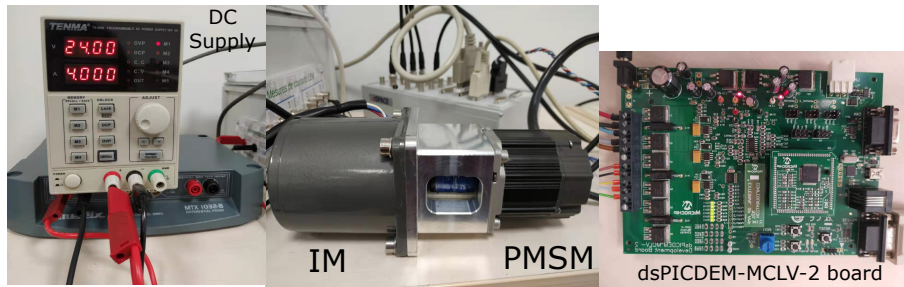


Figure 14: Test-bench.

as on simulation. The torques with and without disturbance compensation are compared in Fig. 17. It can be seen that the torque ripple has been decreased with disturbance compensation. Note that a band pass filter can be used eventually to reduce the static error on  $d_d$  and  $d_q$  and the noise effect to improve the disturbance compensation performance.

The first experimental results on the laboratory test-bench validate the proposed concept. Further tests will be performed on a larger machine as for the previous simulations.

## 6. Conclusion

In this paper, a LPV observer has been designed for an induction machine subject to control voltage disturbances induced by inverter supply disturbance. The disturbances are modeled as a part of the state-space vector in an extended state-space model. The observer gain is determined off-line by a numerical convex optimization. The observer is easy to implement, and its on-line computational cost is smaller than that of an extended Kalman filter. Thanks to this observer, it should be possible to compensate for the disturbances without adding sensors and without changing the main control law. It can be used on the same time with other disturbance suppression methods such as robust control. Simulation results show the feasibility of the proposed observer and the disturbance compensation method. The experimental results obtained on a laboratory test-bench confirm the simulation report. Since there is current noise, the validation of our approach on the laboratory test-bench corresponds to a realistic case study. The proposed observer can be extended to other type of motor drives and can be used to compensate other sinusoidal disturbances whose frequency is known, such as acoustic noise of machine.

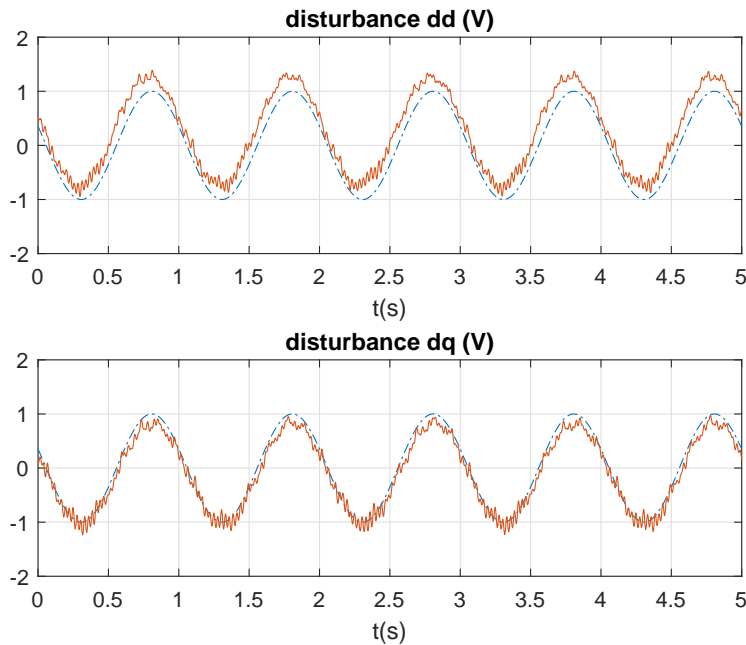


Figure 15: Experimental results for speed of 100 rpm.

Future works will focus, on the one hand, on improving parameter identification of the used motor in order to perform more experimental test; on the other hand, it will look at the possibility of improving the robustness of the observer by more sophisticated convex design techniques. The possibility of taking into account non-sinusoidal disturbances will be considered as well.

## References

- [1] Y. Liu, Y. Sun, M. Su, M. Zhou, Q. Zhu, and X. Li, “A single-phase pfc rectifier with wide output voltage and low-frequency ripple power decoupling,” *IEEE Transactions on Power Electronics*, vol. 33, no. 6, pp. 5076–5086, 2018.
- [2] M. Geoffriault, E. Godoy, D. Beauvois, and G. Favennec, “Active reduction of vibrations in synchronous motors by use of an estimator,” in *2013 IEEE International Conference on Control Applications (CCA) Part of 2013 IEEE Multi-Conference on Systems and Control*, Hyderabad, India, 2013.

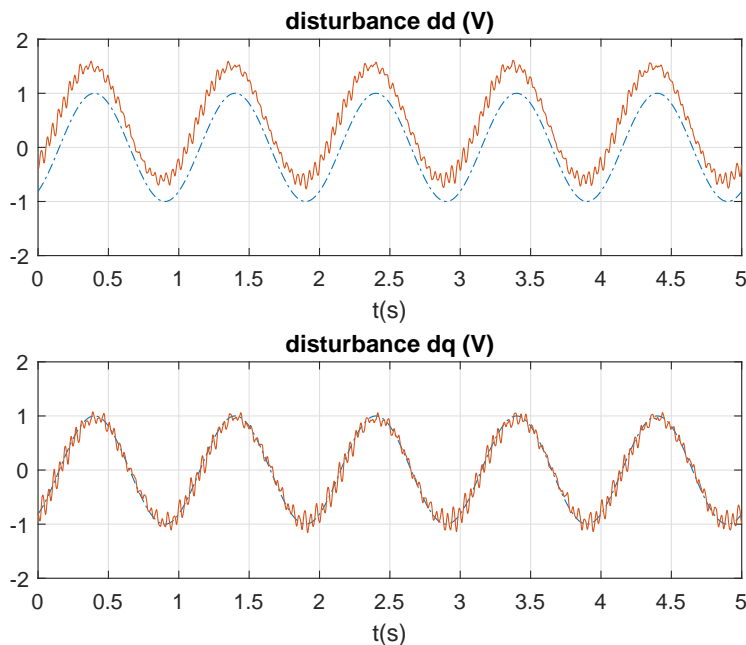


Figure 16: Experimental results for speed of 200 rpm.

- [3] S. Tebbani, E. Godoy, K. Sauterau, and Y. Louvin, “Synchronization of the inverter voltage supply in order to reduce the residual output ripple,” in *EPE2003-10th European Conference on Power Electronics and Applications*, Toulouse, France, 2003.
- [4] P. Ballesteros, X. Shu, W. Heins, and C. Bohn, “LPV gain-scheduled output feedback for active control of harmonic disturbances with time-varying frequencies,” in *Advances on Analysis and Control of Vibrations-Theory and Applications*. IntechOpen, 2012.
- [5] M. Hilaiet, C. Darengosse, F. Auger, and P. Chevrel, “Synthesis and analysis of robust flux observers for induction machines,” in *IFAC Proceedings*, vol. 33, no. 14, 2000, pp. 573–578.
- [6] J. C. Geromel and M. C. de Oliveira, “ $H_2$  and  $H_\infty$  robust filtering for convex bounded uncertain system,” *IEEE Trans. Automatic Control*, vol. 40, no. 1, pp. 100–107, 2001.

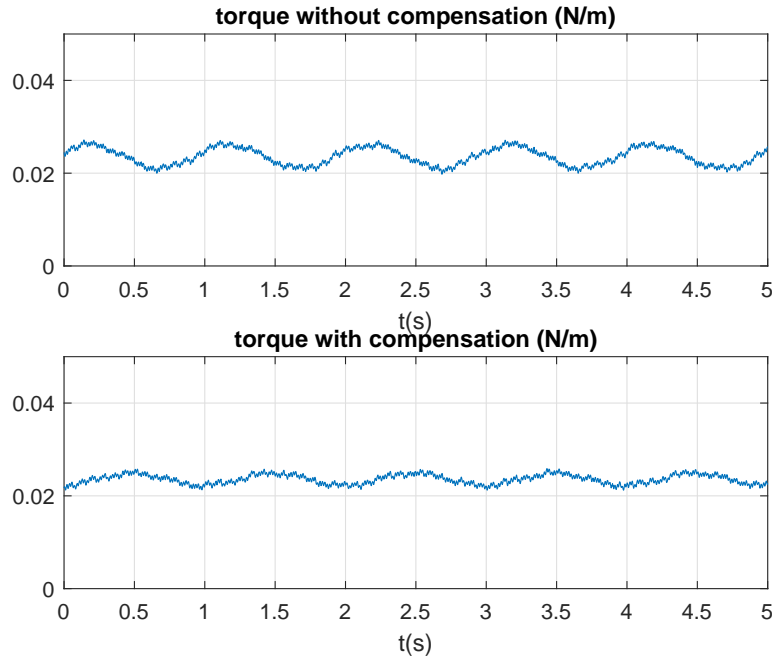


Figure 17: Comparison of the torque with and without disturbance compensation.

- [7] R. Meneceur, A. Metatla, and N. Meneceur, “State space modeling theory of induction motors for sensorless control and motoring purposes,” pp. 481–496, 2012.
- [8] B. Singh, B. N. Singh, A. Chandra, K. Al-Haddad, A. Pandey, and D. P. Kothari, “A review of single-phase improved power quality acdc converters,” *IEEE Transactions Ind. Power Electronics*, vol. 50, no. 5, pp. 962–981, 2003.
- [9] S. Evanczuk, *Power Factor Correction Maximizes Power Efficiency and Quality in Energy-Harvesting Systems*, 2013. [Online]. Available: <https://www.digikey.fr/fr/articles/power-factor-correction-maximizes-power-efficiency-and-quality-in-energy-harvesting-systems>
- [10] R. Kalman, “Contributions to the theory of optimal control,” *Bol. Soc. Mat. Mexicana*, vol. 5, no. 2, pp. 102–119, 1960.
- [11] J. Shamma and M. Athans, “Guaranteed properties of gain scheduled

- control for linear parameter-varying plants,” *Automatica*, vol. 27, no. 3, pp. 559–564, 1991.
- [12] F. Bruzelius, “Linear parameter varying systems,” Ph.D. dissertation, Chalmers University of Technology, 2004.
- [13] M. Chilali, P. Gahinet, and P. Apkarian, “Robust pole placement in lmi regions,” *IEEE transactions on Automatic Control*, vol. 44, no. 12, pp. 2257–2270, 1999.
- [14] S. Boyd, L. El Ghaoui, E. Feron, and V. Balakrishnan, *Linear matrix inequalities in system and control theory*. Siam, 1994, vol. 15.
- [15] MOSEK ApS, *The MOSEK optimization toolbox for MATLAB manual. Version 8.1.*, 2017. [Online]. Available: <http://docs.mosek.com/8.1/toolbox/index.html>
- [16] J. Löfberg, “Yalmip: A toolbox for modeling and optimization in matlab,” in *In Proceedings of the CACSD Conference*, Taipei, Taiwan, 2004.
- [17] R. Gabriel, W. Leonhard, and C. Nordby, “Field-oriented control of a standard ac motor using microprocessors,” *IEEE Transactions on Industry Applications*, vol. IA-16, pp. 186–192, 1980.